

# *Boron Nitride Nanotube Mat as a Low-k Dielectric Material with Relative Dielectric Constant Ranging from 1.0 to 1.1*

**Xinghua Hong, Daojun Wang & D. D. L. Chung**

**Journal of Electronic Materials**

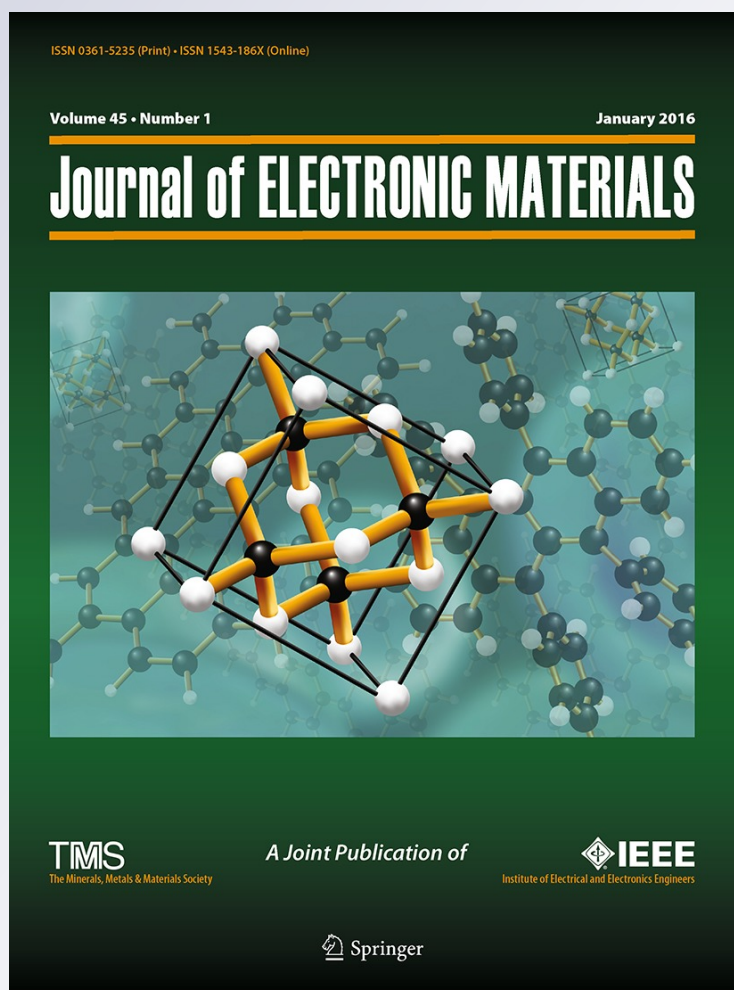
ISSN 0361-5235

Volume 45

Number 1

Journal of Elec Materi (2016) 45:453-461

DOI 10.1007/s11664-015-4123-8



**Your article is protected by copyright and all rights are held exclusively by The Minerals, Metals & Materials Society. This e-offprint is for personal use only and shall not be self-archived in electronic repositories. If you wish to self-archive your article, please use the accepted manuscript version for posting on your own website. You may further deposit the accepted manuscript version in any repository, provided it is only made publicly available 12 months after official publication or later and provided acknowledgement is given to the original source of publication and a link is inserted to the published article on Springer's website. The link must be accompanied by the following text: "The final publication is available at [link.springer.com](http://link.springer.com)".**

# Boron Nitride Nanotube Mat as a Low- $k$ Dielectric Material with Relative Dielectric Constant Ranging from 1.0 to 1.1

XINGHUA HONG,<sup>1,2</sup> DAOJUN WANG,<sup>2</sup> and D.D.L. CHUNG<sup>2,3</sup>

1.—Key Laboratory of Textile Science & Technology, College of Textile, Donghua University, Shanghai 201620, China. 2.—Composite Materials Research Laboratory, University at Buffalo, State University of New York, Buffalo, NY 14260-4400, USA. 3.—e-mail: ddlchung@buffalo.edu

This paper reports that a boron nitride nanotube (BNNT) mat containing air and 1.4 vol.% BNNTs is a low- $k$  dielectric material for microelectronic packaging, exhibiting relative dielectric constant of 1.0 to 1.1 (50 Hz to 2 MHz) and elastic modulus of 10 MPa. The mat is prepared by compacting BNNTs at 5.8 kPa. This paper also presents measurements of the dielectric properties of BNNTs (mostly multiwalled). The relative dielectric constant of the BNNT solid in the mat decreases with increasing frequency, with attractively low values ranging from 3.0 to 6.2; the alternating-current (AC) electrical conductivity increases with increasing frequency, with attractively low values ranging from  $10^{-10}$  S/m to  $10^{-6}$  S/m and an approximately linear relationship between log conductivity and log frequency. The specific contact capacitance of the interface between BNNTs and the electrical contact decreases with increasing frequency, with attractively high values ranging from  $1.6 \mu\text{F}/\text{m}^2$  to  $2.3 \mu\text{F}/\text{m}^2$ . The AC electrical resistivity of the BNNT–contact interface decreases with increasing frequency, with high values ranging from  $0.14 \text{ M}\Omega \text{ cm}^2$  to  $440 \text{ M}\Omega \text{ cm}^2$ .

**Key words:** Boron nitride nanotubes, electrical conductivity, dielectric constant, permittivity, low- $k$  dielectric

## List of Symbols

$A$  Specimen area ( $\pi \times 15.85 \times 15.85 \text{ mm}^2$ )  
 $C$  Measured capacitance for the specimen (BNNT mat)  
 $C_i$  Capacitance of the interface between the specimen and each of the electrical contacts  
 $C_{ib}$  Capacitance of the interface between the BNNT (solid) and an electrical contact  
 $C_{ia}$  Capacitance of the interface between air in the BNNT mat and an electrical contact  
 $\kappa$  Relative dielectric constant of the specimen (BNNT mat)  
 $R$  AC resistance between the two electrical contacts that sandwich the specimen  
 $R_s$  AC volume resistance of the specimen (BNNT mat)  
 $R_i$  AC resistance of the interface between the specimen and an electrical contact

$R_{ib}$  AC resistance of the interface between the BNNT (solid) and an electrical contact  
 $R_{ia}$  AC resistance of the interface between air and an electrical contact  
 $R_a$  AC volume resistance of the air in the BNNT mat  
 $\rho_i$  AC interfacial resistivity between the specimen and an electrical contact  
 $\rho_{ib}$  AC interfacial resistivity between the BNNT (solid) and an electrical contact  
 $\sigma_b$  AC conductivity of the BNNT (solid)  
 $V_b$  Volume fraction of BNNT (solid) in the BNNT mat  
 $a_b$  Area fraction of the mat that is BNNT (solid)  
 $l$  Specimen thickness  
 $\epsilon_0$  Permittivity of free space ( $8.85 \times 10^{-12} \text{ F/m}$ )

## INTRODUCTION

Dielectric materials with low values of relative dielectric constant (i.e., relative permittivity) are

known as low- $k$  dielectrics,<sup>1,2</sup> being critically needed for substrates, interlevel insulation,<sup>3</sup> and intralevel insulation<sup>4</sup> in microelectronics for the purpose of minimizing signal propagation delays. Such delays are due to capacitance associated with electrical insulators used along with electrical conductors in microelectronic packages.

Low- $k$  dielectrics generally use porosity to achieve low values of relative dielectric constant. Among polymers, the lowest reported value of relative dielectric constant is 1.7, achieved in porous polymers.<sup>1,2</sup> Among ceramics, the lowest reported value is 1.02 at 100 kHz for boron nitride foam of density 1.6 mg/cm<sup>3</sup> (0.07 vol.% hexagonal BN for a BN true density of 2.278 g/cm<sup>35</sup>), obtained by chemical vapor deposition on a nickel foam template that was subsequently removed.<sup>6</sup> However, the foam is stiff and not amenable for the shaping that is necessary for use as a low- $k$  dielectric in electronic packages. The next lowest value of 2.0 is given by fumed alumina compacts.<sup>7</sup> Ceramics tend to be superior to polymers in terms of thermal conductivity and ability to withstand elevated temperature. This paper is directed at providing a low- $k$  dielectric with a lower value of relative dielectric constant than all previously reported polymeric or ceramic low- $k$  dielectrics (other than BN foam). Indeed, exceptionally low values ranging from 1.0 and 1.1 (50 Hz to 2 MHz) have been achieved in this work, with the material being boron nitride nanotube (BNNT) mats.

BNNTs have received considerable attention recently due to their combination of high thermal conductivity, low dielectric constant, and high modulus of elasticity.<sup>8–10</sup> At room temperature, the thermal conductivity of a multiwalled BNNT can be comparable to that of a multiwalled carbon nanotube (CNT) and may exceed it if made isotopically pure.<sup>10</sup> The main difference between BNNTs and CNTs is that BNNTs are electrically nonconductive, whereas CNTs are electrically conductive. The combination of low electrical conductivity and high thermal conductivity is not common among materials; diamond is the primary example of a material that exhibits this combination of properties. This combination of properties is valuable for heat dissipation from microelectronic packages, which commonly suffer from overheating.

Another attractive property exhibited by BNNTs is a relatively low value of relative dielectric constant; a value of 5.90 has been predicted by calculation.<sup>8</sup> The combination of high thermal conductivity and low relative dielectric constant is not common among electrically nonconductive materials; For example, polymers tend to have low values of relative dielectric constant, but relatively low values of thermal conductivity; ceramics tend to have higher thermal conductivity, but also higher values of relative dielectric constant. Applications of electrical insulators in electronic packaging include as encapsulation, interlayer dielectrics, printed circuit boards, electric cable jackets, etc. With heat

dissipation and high-speed signal propagation being critically important for enhancing the reliability, power, performance, and further miniaturization of microelectronics, materials that exhibit the combination of high thermal conductivity, low dielectric constant, and low electrical conductivity are much needed.

Nanotubes are commonly used in the form of mats or yarns. A mat or yarn consists of a number of nanotubes that are weakly held together by van der Waals forces. There is no matrix material, so that a mat or yarn includes a lot of air voids. A small amount of binder may or may not be present to hold the nanotubes together at their junctions.

A yarn is a filament in which the nanotubes have preferred orientation along the filament axis. A mat is a sheet in which the nanotubes most commonly have preferred orientation in the plane of the sheet, such that the nanotubes are randomly oriented in the plane of the sheet. The in-plane preferred orientation stems from the pressure used to compact the nanotubes during fabrication of the mat.

This paper addresses both BNNT solid and BNNT mat in relation to the dielectric and electrical conduction properties. The low values of relative dielectric constant of both solid and mat, as found in this work, are valuable not only for electronic packaging, but also for low-voltage cell electroporation.<sup>11</sup>

Addition of BNNTs to epoxy increases the thermal conductivity greatly and decreases the relative dielectric constant slightly.<sup>12,13</sup> The electrical conductivity is decreased by BNNT addition, an effect that diminishes as the frequency is increased.<sup>12</sup> However, the effect on the dielectric properties is not consistently reported in the literature. Reference 12 reports that the dielectric loss is decreased by BNNT addition (10 wt.% to 30 wt.% BNNTs), whereas Ref. 13 reports that the dielectric loss is increased by BNNT addition (1 wt.% to 5 wt.% BNNTs). The relative dielectric constant decreases with increasing frequency,<sup>12,13</sup> as expected. However, Ref. 12 reports that the effect of BNNT addition on the relative dielectric constant diminishes with increasing frequency, whereas Ref. 13 reports that the BNNT effect intensifies with increasing frequency. Moreover, the imaginary part of the relative dielectric constant has not been previously reported. Although the effects of BNNT addition to epoxy have been studied by measuring the properties of the resulting epoxy-matrix BNNT composites,<sup>12,13</sup> the properties of the BNNTs themselves have not been determined. In addition, the relative dielectric constant was determined with inclusion of the capacitance associated with the electrical contacts with that of the specimen, so that the measured capacitance from which the relative dielectric constant was calculated included the contribution from the electrical contacts.<sup>12,13</sup>

This work aims to provide a low- $k$  dielectric material with an exceptionally low value of relative



dielectric constant. In addition, it aims to present experimental characterization of the dielectric properties of BNNT solid and mat, involving determination of the relative dielectric constant and alternating-current (AC) electrical conductivity, including their frequency dependence. The rigor of the above-mentioned experimental characterization partly stems from the fact that the determination of the relative dielectric constant and AC electrical conductivity involves exclusion of the capacitance/resistance associated with the electrical contacts from that of the specimen. This exclusion is enabled by testing each type of material at three different thicknesses. Due to the need for low- $k$  dielectrics to offer adequate mechanical integrity, this work also evaluates the mechanical behavior.

## EXPERIMENTAL PROCEDURES

### Materials

BNNT material was provided by BNNT, LLC (Newport News, VA). These tubes are synthesized using the high-temperature/high-pressure (HTP) method, also called the pressurized vapor/condenser (PVC) method. This method produces highly flexible, high-aspect-ratio BNNTs with high crystallinity. According to the manufacturer, the number of walls in a nanotube typically ranges from 1 to 5, with 2 and 3 being the most common; the tube length is up to 200  $\mu\text{m}$ ; the specific surface area is up to 300  $\text{m}^2/\text{g}$ ; there are up to five BNNTs across each BNNT bundle; the purity is up to 40 wt.% to 50 wt.%; the impurities are in the form of hexagonal BN flakes and elemental boron microdroplets; the as-grown material has a cotton-like appearance, with an unusually low tap density of about 0.25  $\text{mg}/\text{cm}^3$ . The true density is taken as  $1.38 \pm 0.12 \text{ g}/\text{cm}^3$ .<sup>14</sup> The value of  $1.38 \text{ g}/\text{cm}^3$  is the only reported measured value of the true density of BNNT. The value is obtained from the measured density of a BNNT polymer-matrix composite. Since there may be porosity in the composite, the value of  $1.38 \text{ g}/\text{cm}^3$  is likely an underestimate. The energy bandgap is 5.7 eV, according to the manufacturer.

BNNT mats were prepared by compaction of BNNTs in the absence of binder at pressure of 5.8 kPa. By varying the mass of BNNTs used and fixing the area occupied by the BNNTs, the thickness of the resulting mat could be controlled. Scanning electron microscopy (SEM) showed that the structure of the mat was vastly dominated by nanotubes, in spite of the presence of particulate impurities (Fig. 1). Due to the discontinuity of the impurities in the structure and the fact that dielectric connectivity enables greater excursion of polarization charges within an electric field cycle, the impurities are not expected to contribute significantly to the polarizability of the mat. An increase in the compaction pressure causes the BNNTs to be more compacted, but the effect of pressure is not addressed in this paper. Fabrication



Fig. 1. SEM image of BNNT mat obtained at compaction pressure of 0.47 MPa.

of the BNNT mat and characterization of its dielectric and conduction properties were conducted in the same container, as described in “[Relative Dielectric Constant Measurement](#)” section.

### Relative Dielectric Constant Measurement

A controlled mass of BNNTs was placed in an electrically nonconductive polymer cylinder (31.8 mm internal diameter, 60 mm height), such that it was sandwiched inside the cylinder by two copper foils (each with diameter of 31.7 mm and thickness of 0.127 mm), serving as electrical contacts for measurement of relative dielectric constant (Fig. 2). The BNNT specimen was electrically insulated from each of the two copper contacts by using a glass fiber fabric reinforced Teflon film (CS Hyde Company, Lake Villa, IL) of thickness 75  $\mu\text{m}$ . The Teflon film is used to minimize the current. Prior to introducing the BNNTs, each foil was bonded to an epoxy piston of diameter 31.7 mm and height 15 mm during fabrication of the piston from epoxy resin, to enhance the mechanical sturdiness of the foil. Each copper foil has an integral extended part that protrudes [through a vertical slot along the height of the cylinder (not shown in Fig. 2)] beyond the circular main part of the foil to serve as an electrical interconnection. A controlled load (a known weight that fits into the cylinder) is applied via the upper piston for the purpose of compacting the BNNTs slightly.

The thickness of the mat was obtained by measuring the vertical distance between selected points in the above-mentioned setup. For each value of load, mats of three thicknesses were obtained by using three different weighed amounts of BNNTs. The compaction pressure was 5.8 kPa, as provided by an applied known weight of 469.8 g. At this pressure, the three mat thicknesses are  $2.25 \pm 0.01 \text{ mm}$ ,  $4.05 \pm 0.01 \text{ mm}$ , and  $6.27 \pm 0.01 \text{ mm}$ . Based on the true density of BNNTs

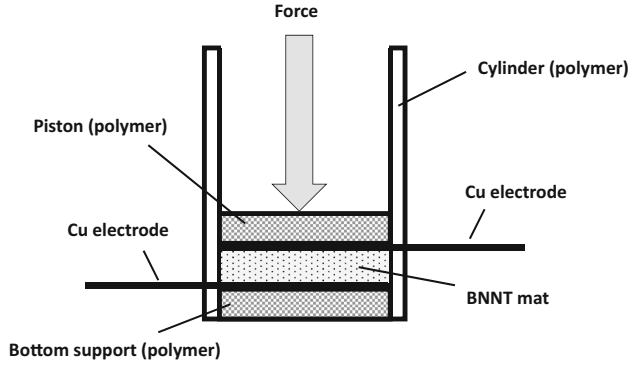


Fig. 2. Schematic illustration of setup for forming and testing BNNT mat in a cylindrical polymer container. Forming involves uniaxial compression using a piston to apply the force. Testing involves using two copper electrical contacts that sandwich the specimen. Each contact has an integral part (leg) that protrudes out of the container. For AC resistance measurement, the specimen is in direct contact with both contacts. For dielectric measurement, the specimen is insulated from the two contacts by using two Teflon films (not shown in the drawing).

( $1.38 \pm 0.12 \text{ g/cm}^3$ <sup>14</sup>) and the density ( $17.36 \pm 0.05 \text{ mg/cm}^3$ ) of the BNNT mat (as measured in this work with the air voids in the mat included in the volume measurement), the BNNT volume fraction in the mat was determined to be  $1.40 \pm 0.10\%$ .

Without removing the BNNT mat from the cylinder after mat formation, the relative dielectric constant was measured with a precision *RLC* meter (Quadtech 7600, Marlborough, MA), using the parallel model for the resistance and capacitance. This model is suitable due to the high resistance of the BNNTs. The compaction pressure is maintained during the measurement, which involves measuring the capacitance at various frequencies scanned from 50 Hz to 2.0 MHz. The AC voltage amplitude applied between the two copper foils for the three thicknesses was 0.5 V, 0.9 V, and 1.4 V, so that the resulting AC electric field amplitude was fixed at 2.2 V/cm. The AC electric field used involves variation in the electric field around an electric field of zero in each cycle of electric field variation.

The measured capacitance  $C$  is for the specimen, including the effect of the two interfaces between the specimen and the two contacts. The two contact interfaces and the specimen are electrically in series. Hence,

$$1/C = 2/C_i + l/(\epsilon_0 \kappa A), \quad (1.)$$

where  $C_i$  is the capacitance due to a specimen–contact interface,  $\epsilon_0$  is the permittivity of free space ( $8.85 \times 10^{-12} \text{ F/m}$ ),  $\kappa$  is the relative dielectric constant of the specimen,  $A$  is the contact area ( $\pi \times 15.85 \times 15.85 \text{ mm}^2 = 789 \text{ mm}^2$ ), and  $l$  is the thickness of the specimen. As shown by Eq. 1,  $C_i$  should be high in order for it to have little influence.

According to Eq. 1,  $1/C$  is plotted against  $l$ <sup>1</sup> (Fig. 3a). The contact capacitance ( $C_i$ ) is the capacitance associated with the interface between the

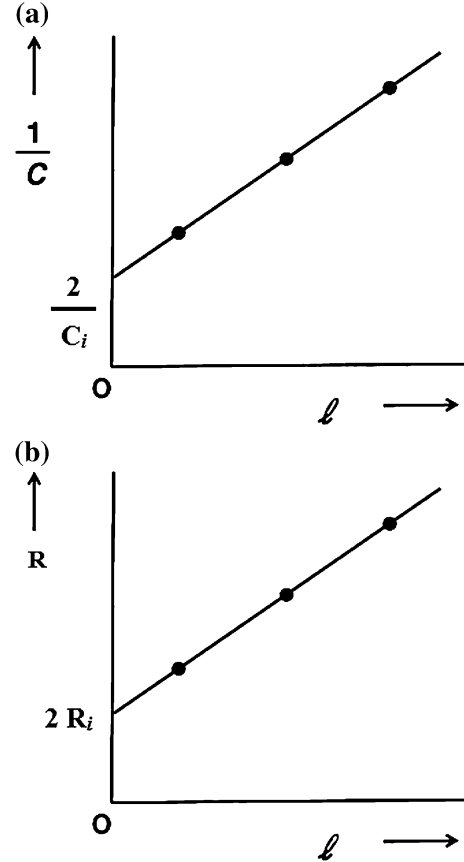


Fig. 3. Schematic plots. On the horizontal axis,  $l$  is the thickness of the specimen. (a) Plot of the reciprocal of the capacitance  $C$  versus thickness  $l$ , for determination of the specimen–contact interfacial capacitance  $C_i$  and the specimen relative dielectric constant  $\kappa$ . The slope equals  $1/(\epsilon_0 \kappa A)$ , where  $A$  is the specimen area and  $\epsilon_0$  is the permittivity of free space. The intercept on the vertical axis equals  $2/C_i$ . (b) Plot of AC resistance  $R$  versus thickness  $l$  for determination of the specimen–contact AC interfacial resistance  $R_i$  and AC volumetric specimen resistance  $R_s$ . The slope equals the AC volumetric specimen resistance  $R_s$  per unit thickness. The intercept on the vertical axis equals  $2R_i$ .

specimen and each of the contacts (Teflon-lined copper) and is included in the measured capacitance ( $C$ ). The value of  $C_i$  is obtained from the intercept of  $2/C_i$  at the  $1/C$  axis at  $l = 0$ , and the value of  $\kappa$  is obtained from the slope, which is equal to  $1/(\epsilon_0 \kappa A)$ .

The specimen is a BNNT mat (consisting of BNNTs and air). The contact capacitance  $C_i$  relates to that of the solid BNNT ( $C_{ib}$ ) and that of air ( $C_{ia}$ ) under the assumption of capacitances in parallel, i.e.,

$$C_i = C_{ib} + C_{ia}. \quad (2)$$

$C_{ia}$  is much smaller than  $C_{ib}$ , because of the air gap effectively corresponding to a relatively large thickness. With the second term neglected, Eq. 2 becomes

$$C_i = C_{ib}. \quad (3)$$

Hence, the specific contact capacitance of the solid–contact interface is given by

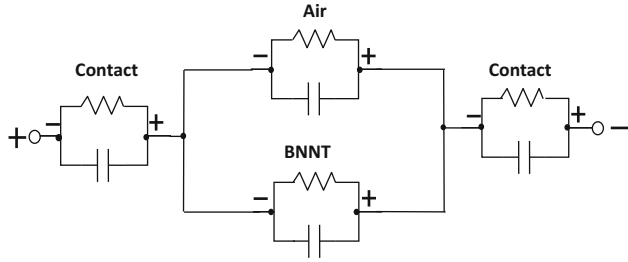


Fig. 4. Equivalent circuit model for BNNT mat. The contact refers to the interface between the mat and the electrical contact.

$$C_{ib}/(a_b A) = C_i/(a_b A), \quad (4)$$

where  $a_b$  is the area fraction of the mat that is solid BNNT.

The relative dielectric constant of the specimen (mat)  $\kappa$  is given by

$$\kappa = \kappa_b V_b + (1 - V_b), \quad (5)$$

where  $\kappa_b$  and  $V_b$  are the relative dielectric constant and the volume fraction of the BNNT solid (with the air voids in the mat excluded). Using Eq. 5,  $\kappa_b$  can be obtained from the measured  $\kappa$ . Due to the very low conductivity and dielectric character of the BNNT, the relative dielectric constant obtained essentially corresponds to the real part of the relative permittivity.

Determination of the BNNT solid/mat properties (as opposed to the composite properties determined in prior work<sup>11,12</sup>) was achieved here by testing BNNT mats (with BNNT and air in a mat) and the use of the equivalent circuit model shown in Fig. 4 for extracting the BNNT solid properties from the BNNT mat properties. All the quantities in the model have been decoupled in this work, in contrast to the absence of any decoupling in prior experimental work. On the other hand, prior theoretical work indicated values of 5.90,<sup>15</sup> 3.6,<sup>16</sup> and 2 to 3<sup>17</sup> for the relative dielectric constant of BNNT in the transverse direction and values ranging from 4.5 to 4.9<sup>16</sup> and from 4.5 to 7<sup>17</sup> in the longitudinal direction.

### AC Electrical Conductivity Measurement

Measurement of the AC electrical conductivity was conducted using the same method as in “Relative Dielectric Constant Measurement” section, except that the Teflon films sandwiching the specimen were removed, so that the specimen was in direct contact with the copper contacts. The same RLC meter, and AC voltage and frequencies were used.

The measured AC resistance  $R$  between the two copper contacts that sandwich the specimen includes the AC resistance  $R_s$  of the specimen and the AC resistance  $R_i$  of each of the two interfaces between the specimen and a copper contact, i.e.,

$$R = R_s + 2R_i. \quad (6)$$

By measuring  $R$  at three specimen thicknesses ( $l$ ), the curve of  $R$  versus thickness is obtained (Fig. 3b). The intercept of this curve with the vertical axis at  $l = 0$  equals  $2R_i$ , whereas the slope of this curve equals  $R_s/l$ , where  $R_s$  is the specimen AC resistance for specimen thickness  $l$ . The specimen AC volume resistivity is obtained by multiplying  $R_s/l$  by the specimen area  $A$ . The AC resistivity of the specimen–contact interface equals the product of  $R_i$  and  $A$ .

The specimen is a BNNT mat. The AC contact resistance  $R_i$  of the interface between the specimen and the copper contact is contributed by the AC contact resistance  $R_{ib}$  of the interface between the BNNT solid and the copper contact and the AC contact resistance  $R_{ia}$  of the interface between the air in the mat and the copper contact. Assuming reasonably (based on the geometry) that these contributions are resistances in parallel,

$$1/R_i = 1/R_{ib} + 1/R_{ia}. \quad (7)$$

With  $R_{ia}$  being essentially infinity, Eq. 7 becomes

$$1/R_i = 1/R_{ib}. \quad (8)$$

The quantity  $R_i$  is obtained from the measured  $R$  for a BNNT mat, using Eq. 6 with the AC volume resistance of the BNNT mat being  $R_s$ , which is given by

$$1/R_s = 1/R_b + 1/R_a, \quad (9)$$

where  $R_b$  is the AC volume resistance of the BNNT solid in the mat and  $R_a$  is the AC volume resistance of the air in the mat. The BNNT and air are considered to be resistances in parallel. Since  $R_a$  is essentially infinity, Eq. 9 becomes

$$1/R_s = 1/R_b. \quad (10)$$

The AC resistance  $R_b$  thus obtained is used to calculate the AC conductivity  $\sigma_b$  of the BNNT solid. The AC interfacial resistivity  $\rho_{ib}$  between the BNNT (solid) and an electrical contact is given by

$$\rho_{ib} = R_{ib} A a_b = R_i A a_b, \quad (11)$$

where  $a_b$  is the fraction of the specimen area that is occupied by the BNNT solid and Eq. 8 has been used.

### Mechanical Testing

Instrumented indentation testing in the form of nanoindentation testing under load control was conducted using a nanoindenter (MTS Systems Corporation, Model XP), equipped with a diamond Berkovich indenter tip with triangle-pyramidal shape and an angle of  $77^\circ$  between the indenter axis and each of the three side-faces of the indenter tip. A high-resolution actuator was used to force the indenter into a test surface, and a high-resolution sensor was used to continuously measure the



resulting penetration. The contact area under load can be inferred from the continuous load–displacement data. Thus, the residual hardness impression (the residual indent) after unloading does not have to be observed, in contrast to conventional hardness testing. The direction of indentation was that of the pressure used in forming the BNNT mat. The maximum load was 10 mN. The load resolution was  $0.05 \mu\text{N}$ . The loading rate was  $1.0 \mu\text{N/s}$ . In each loading cycle, the maximum load was held for 3 s before unloading; the displacement in this period is due to creep. Testing was performed at three different points on the same BNNT mat with thickness of  $0.938 \pm 0.005 \text{ mm}$ .

The elastic modulus  $E$  of the specimen was determined from the reduced modulus,  $E_r$ , obtained from the equation\*

$$E_r = \frac{S\sqrt{\pi}}{2\beta\sqrt{A}}, \quad (12)$$

where  $S$  (known as the contact stiffness, i.e., the stiffness of the indenter–specimen contact) is the slope of the initial portion of the curve of load versus displacement during unloading,  $\beta$  is a constant that depends only on the geometry of the indenter tip ( $\beta = 1.034$  for the Berkovich tip used), and  $A$  is the projected contact area. The specimen modulus  $E$  is then obtained using the equation

$$\frac{1}{E_r} = \frac{(1 - \nu^2)}{E} + \frac{(1 - \nu_i^2)}{E_i}, \quad (13)$$

where  $E_i$  and  $\nu_i$  are the elastic modulus and Poisson's ratio of the indenter tip ( $E_i = 1141 \text{ GPa}$  and  $\nu_i = 0.07$  for the diamond indenter tip used).  $\nu$  is the Poisson's ratio of the specimen (taken as 0.35, which is for single-walled BNNT<sup>18</sup>).

## RESULTS AND DISCUSSION

### Dielectric Properties

Figure 5 shows representative plots akin to those in Fig. 3. The plots are linear, as expected.

Figure 6a shows that the relative dielectric constant of the BNNT solid decreases with increasing frequency, as expected, with values ranging from 3.0 to 6.2. This range is in line with the values of 5.90<sup>15</sup> and 3.6<sup>16</sup> previously predicted by calculation. It is also in line with the values ranging from 2.2 to 6.0 previously reported for boron nitride (not BNNT).<sup>19</sup>

The very low values of relative dielectric constant for the BNNT mat (density  $17.36 \pm 0.05 \text{ mg/cm}^3$ ), which contains air and 1.4 vol.% BNNT solid, range from 1.07 at 50 Hz to 1.03 at 2 MHz, as shown in Fig. 6b. The values are close to the value of 1.02 previously reported at 100 kHz for BN foam (not

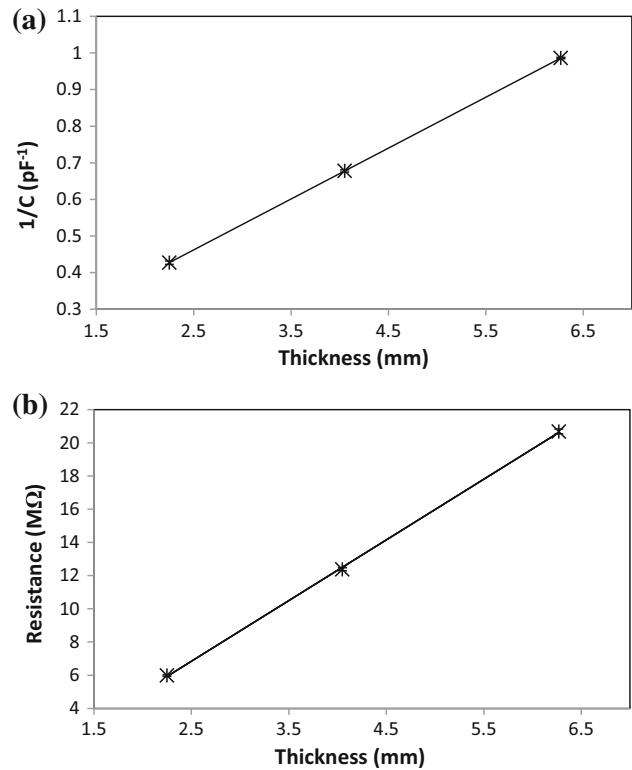


Fig. 5. Experimental results for decoupling the volumetric and interfacial contributions of the BNNT mat (the specimen). (a) Plot of the reciprocal of the measured capacitance (2.0 MHz) versus the specimen thickness. The slope is inversely related to the relative dielectric constant of the specimen. (b) Plot of the measured AC resistance  $R$  (2.0 MHz) versus the specimen thickness. The slope is related to the AC resistivity of the specimen.

BNNT) of density  $1.6 \text{ mg/cm}^3$  (0.07 vol.% hexagonal BN for a BN true density of  $2.278 \text{ g/cm}^3$ ), obtained by chemical vapor deposition on a nickel foam template that was subsequently removed.<sup>6</sup> In spite of the relatively high solid volume fraction (1.4%) of the BNNT mat compared with the BN foam (0.07%), the relative dielectric constant is similar for the two materials. This suggests that the relative dielectric constant of the BN solid in the BN foam is higher than that of the BNNT solid. This difference is consistent with the fact that BNNT includes a hollow air channel, which is absent in BN. However, this difference may also be due to the difference in dielectric connectivity and material preparation method. The connectivity of the BN in the foam may be superior to that in the BNNT mat, and greater dielectric connectivity is expected to enhance the polarization. The scientific origin of the difference in dielectric behavior between the BNNT mat of this work and the BN foam of prior work<sup>6</sup> is not adequately clear.

Figure 7 shows that the specific contact capacitance of the interface between BNNT solid and the electrical contact (Teflon-lined copper) decreases with increasing frequency, with values ranging from  $1.6 \mu\text{F/m}^2$  to  $2.3 \mu\text{F/m}^2$ . These values are large

\*<http://www.msm.cam.ac.uk/mechtest/docs/XP%20User's%20Manual.pdf>, p. 29, as viewed on January 24, 2014.



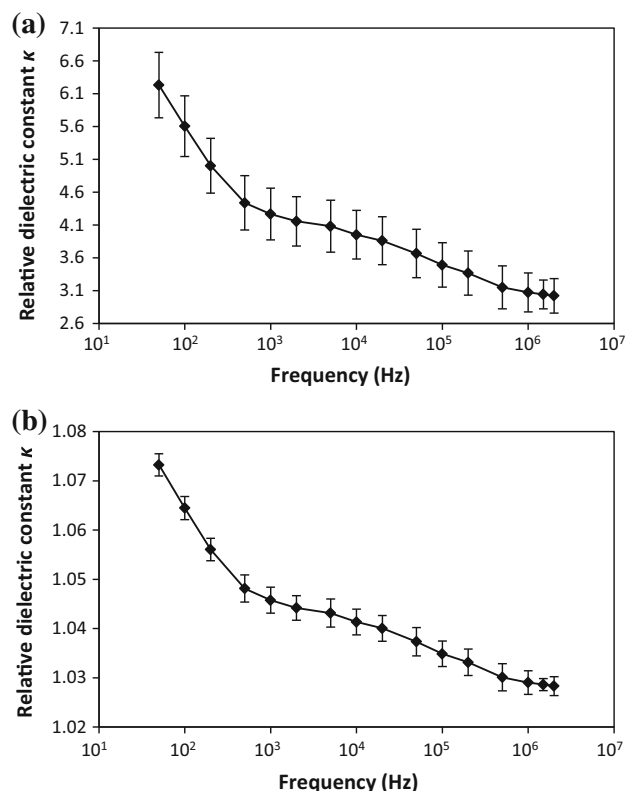


Fig. 6. Plot of relative dielectric constant versus frequency (log): (a) BNNT solid, (b) BNNT mat (consisting of air and BNNT solid). The error in (a) is mainly due to the error in the true density of BNNT.

compared with those of carbon materials; For example, the value for carbon black is  $0.12 \mu\text{F}/\text{m}^2$  and the value for activated carbon is  $0.04 \mu\text{F}/\text{m}^2$ .<sup>20</sup> Since a large value of specific contact capacitance corresponds to a small influence of the contact on the overall (measured) capacitance, this trend means that the contact becomes more influential as the frequency increases. Since the relative dielectric constant decreases with increasing frequency (Fig. 6), the volumetric capacitance decreases with increasing frequency. Thus, the fractional contribution of the contact to the measured capacitance increases with increasing frequency, due to the trends in both Figs. 6 and 7.

Figure 8a shows that the AC conductivity of the BNNT solid increases with increasing frequency, with values ranging from  $10^{-10}$  S/m to  $10^{-6}$  S/m, such that the increase is sharp at frequencies above 0.1 MHz. The corresponding AC resistivity ranges from  $10^8 \Omega \text{ cm}$  to  $10^{12} \Omega \text{ cm}$ . At the lowest frequency of 50 Hz, the AC conductivity is  $2.2 \pm 0.1 \times 10^{-10}$  S/m, which is very low, consistent with the fact that BNNT is a dielectric material; this corresponds to the AC resistivity of  $5 \times 10^{11} \Omega \text{ cm}$ . The observed increase of the AC conductivity with increasing frequency is consistent with the notion that the AC conductivity of a dielectric material is actually the effective conductivity associated with the dielectric polarization. The AC resistivity values

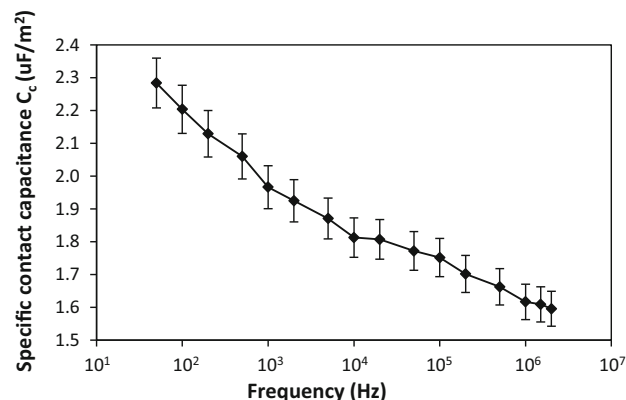


Fig. 7. Plot of specific contact capacitance ( $C_c$  per unit area) of the interface between BNNT solid and the electrical contact versus frequency (log).

ranging from  $10^8 \Omega \text{ cm}$  to  $10^{12} \Omega \text{ cm}$  for the BNNT solid are lower than the DC values ranging from  $1 \times 10^{14} \Omega \text{ cm}$  to  $4 \times 10^{15} \Omega \text{ cm}$  previously reported for hexagonal BN (not BNNT).<sup>21</sup> However, this comparison is not very meaningful.

Figure 9 shows that the AC interfacial resistivity at the interface between the BNNT solid and the electrical contact (copper) decreases with increasing frequency, with values ranging from  $0.14 \text{ M}\Omega \text{ cm}^2$  to  $440 \text{ M}\Omega \text{ cm}^2$ . These values are much greater than the values for carbon materials, e.g.,  $1.1 \Omega \text{ cm}^2$  and  $164 \Omega \text{ cm}^2$  for carbon black and activated carbon, respectively.<sup>20,22</sup> This is consistent with the fact that carbon materials are much more conductive than BNNT. The interfacial resistivity tends to be smaller when the volume resistivity of the contacting parties are lower.

## Mechanical Properties

In spite of the absence of a binder, the BNNT mat remained intact upon being handled by hand and was flexible. Figure 10 shows the nanoindentation results for the BNNT mat. The smoothness of the load versus displacement curve (i.e., the absence of discontinuities) indicates that the indentation mechanism involves sliding of nanotubes relative to one another rather than breaking of nanotubes. Nanotube fracture would have caused one or more discontinuities in the curve. The deformation is partly reversible upon unloading, as shown by Fig. 10. In Fig. 10, the maximum indentation depth ( $28,000 \text{ nm} = 28 \mu\text{m}$ ) corresponds to an indent size under load of  $120 \mu\text{m}$  from the center of the indent. This large lateral indent size means that the indentation was directed at an area that includes a large number of nanotubes. The nanotubes in this area move with respect to one another in response to the indentation, without breaking. This behavior is consistent with the flexibility of the mat.

The modulus, as determined upon unloading at the maximum load, was found to be  $10 \pm 1 \text{ MPa}$ .

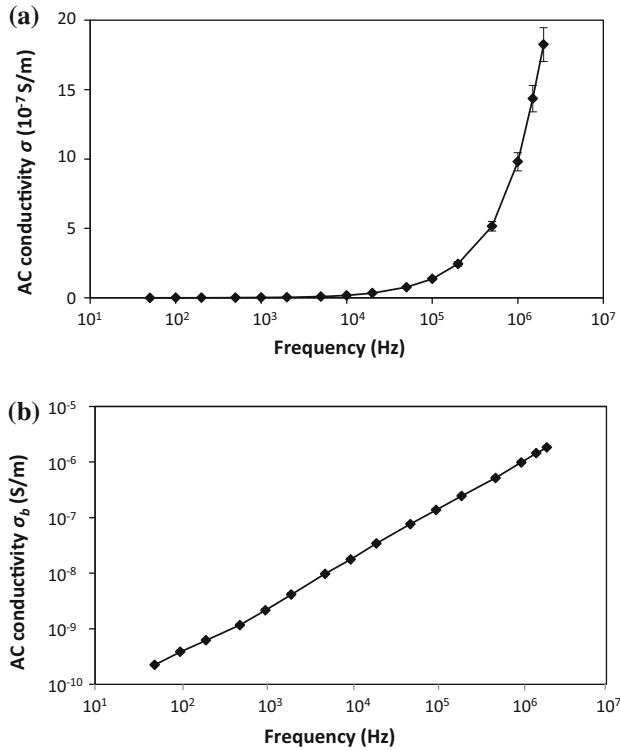


Fig. 8. AC conductivity versus log frequency for the BNNT solid: (a) AC conductivity, (b) log AC conductivity.

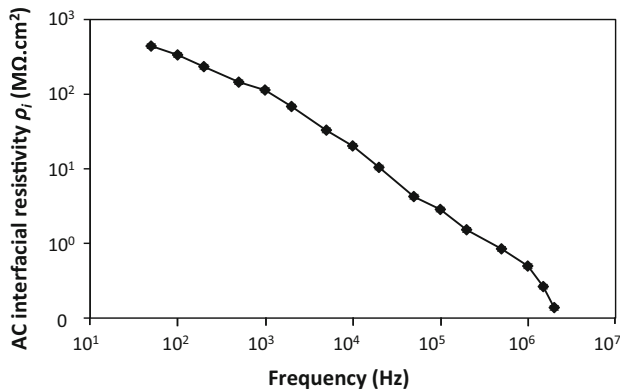


Fig. 9. Plot of AC interfacial resistivity  $\rho_i$  between BNNT solid and a copper electrical contact versus frequency (log).

This value is comparable to that of rubber at small strain<sup>\*\*</sup> and is much lower than the transverse modulus of 30 GPa for a single BNNT (i.e., a single nanotube)<sup>18</sup> and much much lower than the longitudinal modulus of 1.2 TPa for a single BNNT.<sup>23</sup> The relatively low modulus of the BNNT mat is due to the weak linkages (involving merely van der Waals forces) between the BNNTs in a mat and the consequent deformation involving mainly the

<sup>\*\*</sup>[http://www.engineeringtoolbox.com/young-modulus-d\\_417.html](http://www.engineeringtoolbox.com/young-modulus-d_417.html), as viewed on August 2, 2015.

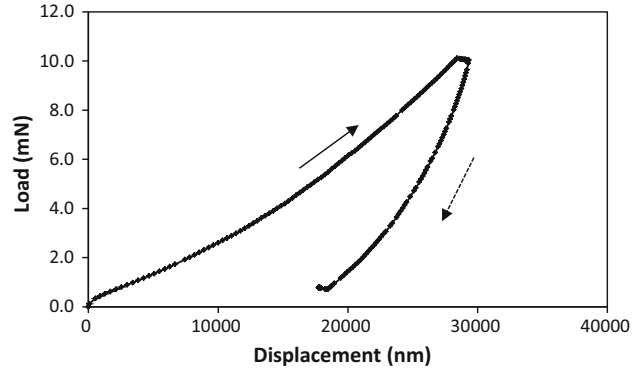


Fig. 10. Curve of load versus displacement obtained during loading and subsequent unloading in nanoindentation testing of the BNNT mat.

movement (such as sliding) of nanotubes relative to one another. The extent of bending of the nanotubes is probably small, if any. On the other hand, the movement renders a degree of viscous character to the mat, as shown by a separate publication by these authors.<sup>24</sup> In other words, the BNNT mat is a ceramic dielectric material that resembles polymeric materials in terms of its mechanical properties. Ceramics tend to be superior to polymers in terms of thermal stability.

## CONCLUSIONS

A boron nitride nanotube (BNNT) mat containing air and 1.4 vol.% BNNT and exhibiting an elastic modulus of  $10 \pm 1$  MPa and density of  $17.4 \text{ mg/cm}^3$  is shown to be a low- $k$  dielectric material with exceptionally low relative dielectric constant of 1.0 to 1.1 (50 Hz to 2 MHz). The material was prepared by uniaxial compaction of BNNTs at 5.8 kPa in the absence of a binder.

The dielectric properties of BNNTs have been experimentally determined. In particular, the dielectric and AC conduction properties of the BNNT solid at frequencies ranging from 50 Hz to 2.0 MHz have been determined, with decoupling of the volumetric and interfacial contributions (the interface being that between the specimen and each electrical contact) and of the contributions from BNNT solid and air in the BNNT mat.

The relative dielectric constant of the BNNT solid decreases with increasing frequency, showing low values ranging from 3.0 to 6.2. The corresponding very low values for the BNNT mat range from 1.07 at 50 Hz to 1.03 at 2 MHz. The specific contact capacitance of the interface between the BNNT solid and the electrical contact decreases with increasing frequency, with high values ranging from  $1.6 \text{ }\mu\text{F/m}^2$  to  $2.3 \text{ }\mu\text{F/m}^2$ . The AC conductivity of the BNNT solid increases with increasing frequency, with low values ranging from  $10^{-10}$  S/m to  $10^{-6}$  S/m, such that the increase is sharp at frequencies above 0.1 MHz and the plot of log conductivity versus log frequency is approximately linear. The AC resistivity of the interface between the

BNNT solid and the electrical contact decreases with increasing frequency, with high values ranging from  $0.14 \text{ M}\Omega \text{ cm}^2$  to  $440 \text{ M}\Omega \text{ cm}^2$ .

All the above-mentioned BNNT solid volumetric properties are attractive for use of BNNT as a dielectric material. The high interfacial capacitance is also attractive. The high interfacial resistivity is not attractive, but the additional resistance provided by the interface is not a problem when the material is used as a dielectric material.

### ACKNOWLEDGEMENTS

The authors thank Dr. Andi Wang and Dr. Yoshihiro Takizawa of University at Buffalo, State University of New York, for technical assistance. They are also grateful to the China Scholarship Council (Beijing, China) for a scholarship provided to one of the authors (Hong). They also thank Professor Cemalettin Basaran of University at Buffalo, State University of New York, for the use of his nanoindenter.

### REFERENCES

1. S. Ma, Y. Wang, Z. Min, and L. Zhong, *Adv. Polymer Technol.* 32, 21358/1 (2013).
2. R. Sasi kumar, M. Ariraman, and M. Alagar, *RSC Adv.* 4, 19127 (2014).
3. S. Lazarouk, S. Katsouba, A. Leshok, A. Demianovich, V. Stanovski, S. Voitech, V. Vysotski, and V. Ponomar, *Microelectron. Eng.* 50, 321 (2000).
4. S. Lazarouka, S. Katsoubaa, A. Demianovich, V. Stanovski, S. Voitech, V. Vysotski, and V. Ponomar, *Solid State Electron.* 44, 815 (2000).
5. R.K. Willardson, A.C. Beer, and M.E. Straumanis *Semiconductors and Semimetals*, Vol. 4, Physics of III–V Compounds (Academic Press, 1968), p. 49.
6. J. Yin, X. Li, J. Zhou, and W. Guo, *Nano Lett.* 13, 3232 (2013).
7. Y. Takizawa and D.D.L. Chung, *J. Electron. Mater.* 44, 2211 (2015).
8. C. Zhi, Y. Bando, C. Tang, and D. Golberg, *Mater. Sci. Eng. R* 70, 92 (2010).
9. S. Kalay, Z. Yilmaz, O. Sen, M. Emanet, E. Kazanc, and M. Culha, *Beilstein J. Nanotechnol.* 6, 84 (2015).
10. C.W. Chang, W. Han, and A. Zettl, *Appl. Phys. Lett.* 86, 173102/1 (2005).
11. V. Raffa, G. Ciofani, and A. Cuschieri, *Nanotechnology* 20, 075104/1 (2009).
12. X. Huang, C. Zhi, P. Jiang, D. Golberg, Y. Bando, and T. Tanaka, *Adv. Funct. Mater.* 23, 1824 (2013).
13. C. Zhi, Y. Chunyi, Y. Bando, T. Terao, C. Tang, D. Golberg, and IUPAC Commission, *Pure Appl. Chem.* 82, 2175 (2010).
14. C. Zhi, Y. Bando, C. Tang, and D. Golberg, *Solid State Commun.* 151, 183 (2011).
15. H. Lan, L. Ye, S. Zhang, and L. Peng, *Appl. Phys. Lett.* 94, 183110/1 (2009).
16. G.Y. Guo and J.C. Lin, *Phys. Rev. B* 71, 165402/1 (2005).
17. G.Y. Guo, S. Ishibashi, T. Tamura, and K. Terakura, *Phys. Rev. B* 75, 245403/1 (2007).
18. S. Govind and S. Bansal, *Int. J. Adv. Mech. Eng.* 4, 331 (2014).
19. J.P. Sullivan, T.A. Friedmann, C.A. Appleby, M.P. Siegal, N. Missert, M.L. Lovejoy, P.B. Mirkarimi, and K.F. McCarty, *Mater. Res. Soc. Symp. Proc.* 381, 273 (1995).
20. A. Wang and D.D.L. Chung, *Carbon* 72, 135 (2014).
21. C. Steinborn, M. Herrmann, U. Keitel, A. Schönecker, J. Räthel, D. Rafaja, and J. Eichler, *J. Eur. Ceram. Soc.* 33, 1225 (2013).
22. X. Hong and D.D.L. Chung, *Carbon* 91, 1 (2015).
23. N.G. Chopra and A. Zettl, *Solid State Commun.* 105, 297 (1998).
24. X. Hong, D. Wang, and D.D.L. Chung, *Composites B*, in press.